Available online at www.sciencedirect.com
ScienceDirect
Biochimica et Biophysica Acta 1777 (2008) 196–201
Biochimica et Biophysica Acta
BBA
www.elsevier.com/locate/bbabio

Redox-coupled proton pumping in cytochrome *c* oxidase: Further insights from computer simulation

Jiancong Xu, Gregory A. Voth *

Department of Chemistry and Center for Biophysical Modeling and Simulation, University of Utah, 315 S. 1400 E., Rm 2020, Salt Lake City, Utah 84112-0850, USA

Received 15 August 2007; received in revised form 12 November 2007; accepted 20 November 2007
Available online 4 December 2007

Abstract

The membrane-bound enzyme cytochrome *c* oxidase, the terminal member in the respiratory chain, converts oxygen into water and generates an electrochemical gradient by coupling the electron transfer to proton pumping across the membrane. Here we have investigated the dynamics of an excess proton and the surrounding protein environment near the active sites. The multi-state empirical valence bond (MS-EVB) molecular dynamics method was used to simulate the explicit dynamics of proton transfer through the critically important hydrophobic channel between Glu242 (bovine notation) and the D-propionate of heme a_3 (PRDa_3) for the first time. The results from these molecular dynamics simulations indicate that the PRDa_3 can indeed re-orientate and dissociate from Arg438, despite the high stability of such an ion pair, and has the ability to accept protons via bound water molecules. Any large conformational change of the adjacent heme a D-propionate group is, however, sterically blocked directly by the protein. Free energy calculations of the PRDa_3 side chain isomerization and the proton translocation between Glu242 and the PRDa_3 site have also been performed. The results exhibit a redox state-dependent dynamical behavior and indicate that reduction of the low-spin heme a may initiate internal transfer of the pumped proton from Glu242 to the PRDa$_3$ site.

Keywords: Cytochrome *c* oxidase; Multi-state empirical valence bond (MS-EVB); Free energy calculation; Proton pumping

1. Introduction

Respiratory heme-copper oxidases constitute the last components of the respiratory chain of most aerobic organisms. These membrane-bound enzymes couple the electron transfer reactions to the proton pumping process across the membrane and catalyze the reduction of dioxygen to water ($O_2 + 8H^+ + 4e^- \rightarrow 2H_2O + 4H^+$). In cytochrome *c* oxidase (C*c*O), an electron is first delivered from cytochrome *c* to the primary electron acceptor, Cu_A, located at the extracellular side of the membrane. From Cu_A, electrons are transferred consecutively to the heme *a* group and to the heme a_3-Cu_B binuclear center where oxygen binds to the Fe of heme a_3.

All protons pumped across the membrane by CcO are transferred through its D-pathway that leads from the cytoplasmic side of the membrane towards the catalytic site. The channel starts at Asp91 near the inner surface of C*c*O, and continues half way into the membrane along a hydrogen-bonded water chain, and ends at the well-conserved Glu242 residue. Glu242 is located ~25 Å above the surface, at approximately equal distances from heme *a* and heme a_3. This residue may undergo a conformational change during the catalytic cycle and facilitates the proton translocation beyond it. Studies of site-directed mutations of the highly conserved arginine pair (Arg438 and Arg439) [1–3], which strongly interact with the D-propionates of the two heme groups via salt bridges (Fig. 1), suggest that the D-propionate of heme a_3 (PRDa_3) is involved in proton pumping and may function as the primary proton acceptor for the pumped protons. It should be noted that throughout this paper bovine CcO notation will be used.

In the crystal structures determined so far there are no water molecules resolved in the hydrophobic cavity beyond Glu242 [4–7], but results from computational studies have suggested

* Corresponding author. Tel. +1 801 581 5419; fax: +1 801 581 4353.
E-mail address: voth@chemistry.utah.edu (G.A. Voth).

0005-2728/$ - see front matter © 2007 Elsevier B.V. All rights reserved.
doi:10.1016/j.bbabio.2007.11.008

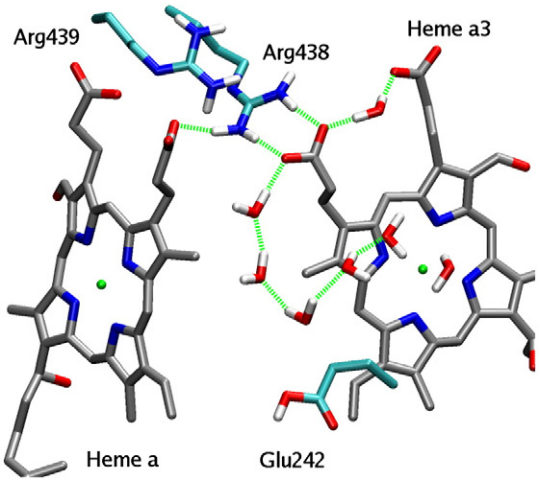

Fig. 1. The hydrogen-bonded, proton-conducting water chains from Glu242 to the D-propionate of heme a_3 and to the binuclear center, as obtained from molecular dynamics simulations. The hydrogen bonds are shown as dashed lines.

[8–11] that the hydrophobic cavity has space to transiently hold several water molecules and those water molecules can form branched chains, connecting Glu242 with the PRDa_3 and the binuclear center (Fig. 1). Indeed, because of their diffusive character, water molecules may not be crystallographically discernible, so some number of water molecules are likely to rearrange themselves during the oxidase cycle. These water molecules are likely to be structurally disordered and the hydrogen-bonded water chains may be formed only transiently during the catalytic cycle.

Although the pathways for the protons to be transported beyond Glu242 have already been suggested, the mechanisms of how the pumped protons and the chemical protons are distinguished and how the alternative proton translocation pathways are regulated by the driving electron transfer reactions are still a matter of debate. A redox state-dependent switch in the orientation of proton translocation (PT) has been proposed to explain this functional duality. A classical molecular dynamics study recently reported by Wikström and coworkers [12,13] has suggested a unique gating mechanism of proton pumping by a redox state-controlled orientation of water arrays in the cavity. However, a complete microscopic understanding of the PT and the validation of these proposed mechanisms can only be achieved through the inclusion of an *explicit* excess proton in the simulation dynamics [14,15]. In the present study, such an effort is made to gain further insight into the proton pumping mechanism in CcO. We focus on the dynamics and the free energy profiles of the excess proton and the surrounding protein environment near the active sites, and in particular, how the proton translocation dynamics from Glu242 to the PRDa_3 site is altered by electron transfer from heme *a* to the binuclear center. The results from our simulations suggest that the proton dynamics close to the active sites and certain protein conformational rearrangements are redox state-dependent. The key role of heme *a* in the proton pumping mechanism is also discussed.

2. Methods

All of the molecular dynamics (MD) simulations presented in this work were performed using the DL_POLY [16] package modified to incorporate the second generation multi-state empirical valence bond (MS-EVB2) algorithm [14,15] and the Amber99 force field [17]. The implementation of the MS-EVB2 methodology for simulations of CcO has been previously described in Refs. [18,19]. The starting structure for the simulations includes both subunit I and II of the bovine cytochrome *c* oxidase (PDB ID code 1v54) [6], crystallographic waters within 8 Å of these two subunits, and an excess proton (constituting a composite system of ~13,000 atoms). A weak harmonic restraint of 1 kcal/mol. Å^2 was applied to the C_α atoms to maintain the shape of the isolated and solvated protein subunits I and II. These restraints were used in previous MD simulations of one subunit of CcO [18,19]. Six water molecules were inserted into the hydrophobic cavity between the two hemes. The residues Glu242 and Asp364 were then protonated, and all heme propionates were deprotonated, as suggested by electrostatic calculations [20]. The rest of the amino acids remained in their default protonation state. Standard electrostatic potential (ESP) derived charges for the Cu_B center, the His240- Tyr244 crosslink, and Cu_B with its three histidine ligands (His290, His291, His240), were calculated with the Hartree–Fock method from *Gaussian 03* using the 6-31G* basis set, and then fitted to the restrained electrostatic potential (RESP) charges used in the Amber99 force field [17,21]. The Cu_B center was assumed to be in its reduced state throughout. The partial charges for heme groups were derived mainly from the ZINDO/1 method in HyperChem (version 7.5, Hypercube, Inc.). If one of the hemes was reduced, its overall charge became one charge unit more negative.

A further truncated system, including only the subunit I, internal water molecules and bulk water within 8 Å of the subunit I, was employed for the free energy profile, i.e., potential of mean force (PMF), calculations to reduce the computational cost. To calculate the PMF for PT between Glu242 and PRDa_3, an internal reaction coordinate was chosen as the position of the center of excess charge [18,22] projected along the direction defined as the vector connecting the center of mass position of the Glu242 C_δ atom to the center of mass position of the Arg438 NH2 atom. The protocol for the PMF calculations has been described elsewhere [18,19] and was followed in the present calculations. A series of umbrella sampling simulations [23,24] was carried out with a window spacing of 0.25 Å and a force constant k=15 ~ 100 kcal/mol. Each window was simulated with an equilibration time of 100 ps and a sampling time of 1.5 ns. The PMF was then constructed from the density distributions in each window via the weighted histogram analysis methods (WHAM) [23]. The simulation trajectories were then analyzed with tools either from the GROMACS package [25,26] or an in-house code. Computer-aided structure analysis was performed using the VMD software [27].

3. Results and discussion

3.1. The Arg438 and PRDa_3 ion pair

The D-propionate of heme a_3 (PRDa_3) forms salt bridges with two arginines (Arg438 and Arg439). Mutagenesis experiments suggest that the D-propionate is a potential proton-loading site for the pumped protons, and is likely involved in the proton exit pathway [1,2]. This PRDa_3 side chain group would be in very good position to receive protons from Glu242 if it undergoes a conformational change such that a PT pathway can be created. However, this view has been challenged based on inspection of the crystal structure [6] in which the PRDa_3 is highly stabilized by the hydrogen bonds and charge interactions with Arg438 and Arg439, making the dissociation of the PRDa_3 and Arg438 pair seem unlikely. Since X-ray studies provide a static picture of the protein, and only limited information about fluctuations within the protein structure, Wikström and coworkers [12] tested this possibility recently by conventional MD simulations and showed that the

hydrogen–oxygen distance of the Arg438/PRDa_3 pair fluctuated to a transient maximum (≈0.1 ps) of >4 Å, indicating that the ion pair can indeed dissociate.

The MD study of Wikström et al. also showed that dissociation of the ion pair is controlled by the oxidation states of heme *a* and the heme a_3-Cu_B binuclear center, indicating a redox state-dependence of the dissociation event [12]. Therefore, to further evaluate the relative thermodynamic stability of the Arg438/PRDa_3 ion pair and to quantitively examine its sensitivity to the different heme and Cu_B oxidation states, free energies were calculated in the present work as a function of the dihedral angle θ (C_α-C_β-C_γ-C_δ) of the PRDa_3 side chain with the enzyme in two different oxidation states: the ORR state, where the binuclear center is fully reduced (two electrons) and the ROR state, where the second electron is on heme *a* rather than on heme a_3, and the results are shown in Fig. 2. The characteristic features of the free energy profiles as the PRDa_3 side chain changing from $\theta = -180°$ to 0° are that both profiles exhibit a considerable increase, but the energy rise is greater in the ORR state than in the ROR state. The results suggest that, first, the most favorable configuration for the PRDa_3 side chain is when it is strongly interacting with Arg438 and, second, that the PRDa_3 side chain can more easily rearrange itself via a downward swing and be ready to receive a proton upon the reduction of heme *a*.

Several MS-EVB2 simulations were also performed with an excess proton at the bottom of the water chain close to Glu242. During the simulations, five water molecules form two hydrogen-bonded paths between Glu242 and the PRDa_3 site or the binuclear center. One water molecule binds to the active site, bridging Fe and Cu, which provides insight into the O_2/water accessibility of the active site (Figs. 1 and 3). In each of these simulations with an explicit excess proton included, considerable fluctuation in the hydrogen-bond network near Arg438 and the PRDa_3 site occurred. Additionally, significant conformational changes were observed for the PRDa_3 side chain; the PRDa_3 group was seen to undergo a rotation an orientation from pointing up towards Arg438 to one pointing downwards to the water chain between hemes (Fig. 3), allowing formation of distinct interactions with the excess proton. It should be noted that in Fig. 3 the excess proton is solvated as a Zundel complex $H_5O_2^+$, shared between two individual water molecules; the Zundel complex is in turn stabilized by hydrogen-bonding (h-bonding) with the carboxylate group of the PRDa_3. The overall h-bonding interactions between the Zundel and the PRDa_3 group became stronger as is evidenced by short distances ranging from 1.3 to 2.0 Å. The formation of a strong ionic h-bonded proton wire is likely to lower the free energy barrier for proton hopping.

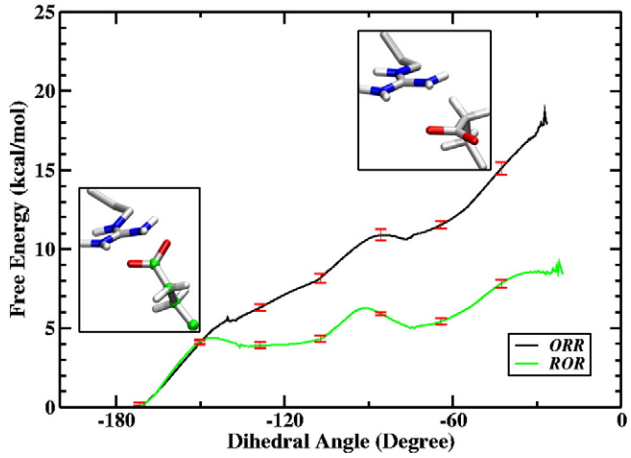

Fig. 2. Free energy profiles (PMFs) for the side chain rotation of the PRDa_3 with the enzyme in two redox states: the ORR state and ROR state. The water molecules are hidden for clarity. The error bars of the profiles range from ±0.1 to 0.4 kcal/mol.

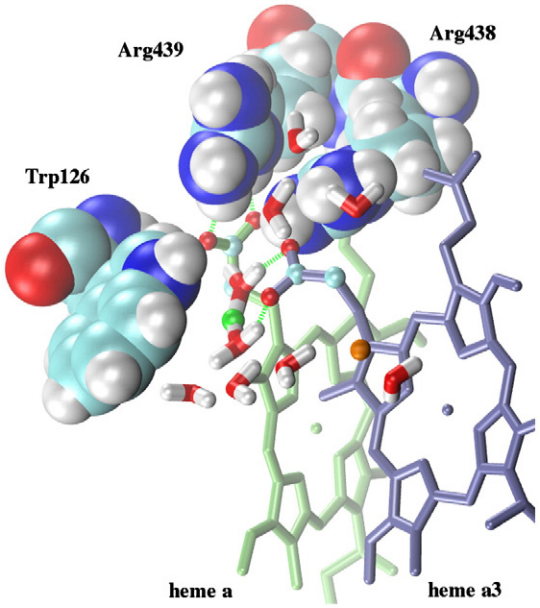

Fig. 3. Snapshot at the end of 150 ps of an MS-EVB2 MD simulation. Dashed lines indicate the H-bonding interactions. The residues are colored by atom name following standard convention. The excess proton is represented as a green sphere, and shared by two water molecules in a Zundel complex $H_5O_2^+$. (For interpretation of the references to color in this figure legend, the reader is referred to the web version of this article.)

The increase of the hydrogen–oxygen distance of the Arg438/PRDa_3 pair has been reported previously in the conventional MD study [12], where the pair was found to be slightly pushed away from each other, but to our knowledge the present results are the first time that such a dramatic downward conformational change of the PRDa_3 side chain has been observed. These results further confirm that the D-propionate of heme a_3 has enough flexibility to change its conformation and coordination as it dissociates from Arg438 and likely accepts protons directly via bound water molecules. This conformational isomerization also allows water exchange between the hydrophobic cavity and the exit channel beyond Arg438, a behavior also revealed in other MD studies [12].

It should be mentioned that although the D-propionate groups of both heme *a* and heme a_3 are buried at the same level inside the protein and proximal to each other, a conformational change of the heme *a* D-propionate was not seen in our simulations. This may be explained by the steric barrier imposed by the surrounding residues, such as Arg438, Arg439 and Trp126

(Fig. 3), as well as the strong tendency to retain the hydrogen-bonded structure. The D-propionate of heme *a* cannot move past these residues without perturbing the protein structure, and thus remained away from the inside of the hydrophobic cavity.

3.2. The proton pumping path between Glu242 and PRDa_3

The translocation of protons from Glu242 to the proton-loading site, presumably the PRDa_3 group near the exit channel, is the expected first step in the directional proton pumping by CcO. To gain further insight into the proton pumping mechanism, and in particular to investigate the energetic consequences of the redox states on the PT from Glu242 to PRDa_3, free energy (PMF) calculations of the proton translocation along the path were performed. The active sites, heme *a*, heme a_3, and Cu_B, were treated in three different redox states: ORR, oxidized heme *a*, and fully reduced heme a_3-Cu_B binuclear center; OOR, oxidized hemes, and reduced Cu_B; and ROR, reduced heme *a*, oxidized heme a_3, and reduced Cu_B. In all the simulations reported here, the Glu242 residue was protonated for reasons that will be described below. The PMFs were constructed using the umbrella sampling technique incorporated in the MS-EVB2 model as described earlier. The PMF in this case is the permeation free energy profile of the excess proton projected on the relevant reaction coordinate (RC) defined along the pathway connecting Glu242 and the PRDa_3 (see Methods section).

The resulting free energy profiles from Glu242 towards the PRDa_3 are shown in Fig. 4. At RC=4 Å, the center of excess charge is located on average above Glu242 near the bottom of the path, whereas RC=10 Å represents a configuration in which the excess proton is located in close vicinity of the PRDa_3/Arg438 pair (see the insets in Fig. 4). The intermediate position, RC=6 Å, corresponds to the intersection of the two

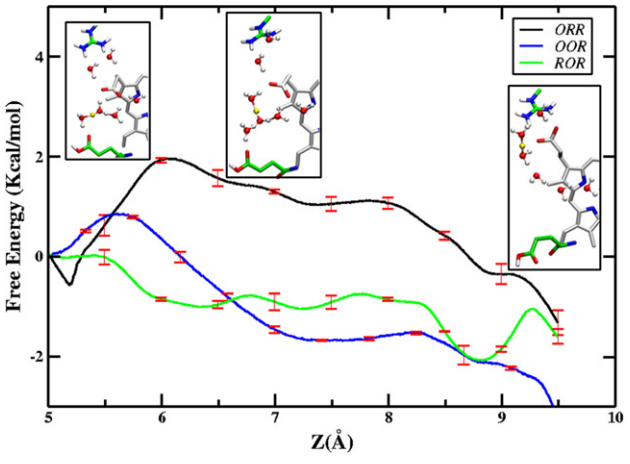

Fig. 4. Free energy profiles (PMFs) for proton translocation along the reaction coordinate of the pathway between Glu242 and D-propionate of heme a_3, with the catalytic sites, heme *a*, heme a_3, and Cu_B, in different oxidation states (see text for details). The error bars of the profiles come from block averaging, and range from ±0.02 to 0.25 kcal/mol. The insets show the transferred proton as a yellow sphere. (For interpretation of the references to color in this figure legend, the reader is referred to the web version of this article.)

branched pathways leading separately to the PRDa_3 site and the binuclear center. The free energy barrier associated with PT in the ORR state is ~2 kcal/mol, with a peak around RC=6 Å; as the heme a_3-Cu_B binuclear center becomes one charge unit less negative, the free energy barrier in the OOR intermediate state appears less pronounced, i.e., less than 1 kcal/mol. With a second electron on heme *a* (the ROR state), however, the profile exhibits an apparent downhill trend, and the proton experiences no barrier in translocating from Glu242 to the PRDa_3 site, indicating a favorable proton movement between them. These results indicate that the PT between Glu242 and the PRDa_3 is less favorable when the binuclear center is fully reduced, and it is therefore conceivable that in this case the proton would be drawn to the binuclear center. In fact, an inspection of the simulation trajectories indicates that the solvation structure of the excess proton is very unstable at RC=6 Å, and a relatively large umbrella force constant was required to constrain the center of excess charge at the equilibrium position in the free energy umbrella sampling for the PMF calculations.

To avoid the unproductive back flow of protons from the extracellular side, the protein must ensure that, following Glu242 deprotonation, the energy barrier for back proton transfer from the PRDa_3 group to Glu242 is larger than that for proton transfer from Glu242 to the PRDa_3 site. The above PMF calculations suggest in response to a second electron on heme *a* the proton released from Glu242 now has a driving force to move close to the PRDa_3 group, which may help to suppress the back proton transfer from the PRDa_3 group to Glu242.

The present work assumes that Glu242 has been rapidly reprotonated after proton dissociation. This was in part necessary given that the current MS-EVB model cannot describe proton transfer between water molecules and a protonatable residue, such as glutamic acid, and in part motivated by the rationale that Glu242 has a pK_a value higher than physiological condition and likely becomes quickly reprotonated after releasing its proton. The second proton could come from the recently discovered "proton trap" region 6–7 Å below Glu242 in the D-pathway [18,19,31], though it could come from other locations as well. However, the acidity of Glu242 may actually depend on the redox states of the metal centers. IR difference spectra studies [28–30] have shown that the protonation state of Glu242 can change upon electron transfer between heme a and the binuclear center, and that Glu242 can be deprotonated under certain circumstances. These studies suggested Glu242's pK_a shift might be caused by conformational changes in protein backbone that alter the microenvironment of the residue and thereby alter proton dissociation. These results seem to contradict the assumption made in the present work, that Glu242 is rapidly reprotonated, and certainly warrant further simulation analysis with a fully protonatable glutamic acid MS-EVB model. It is not clear, however, if the experimentally observed states are long lived or transiently formed during transitions. Thus, further experimental studies are likely also necessary to elucidate the sequence and timescale of protonation events of key residues, such as Glu242, PRDa_3 and Arg438, and the complex electron/proton linkage before the vectorial proton pumping mechanism can be thoroughly understood.

Despite these open-ended questions, the present study seeks to clarify which oxidation states enable the proton released from Glu242 to favor the putatitive pump-loading site, $PRDa_3$, over the binuclear center. This study is not addressing the full proton transfer process from Glu242 to $PRDa_3$, which would clearly involve a rate-limiting barrier of dissociation (explaining the long timescales associated with this transfer). These issues will be the focus of future work.

The MS-EVB2 model used in the current study is also not currently capable of completely delocalizing the proton on the PRDa_3 side chain through a dynamical protonation/deprotonation event. Including a protonatable PRDa_3 side chain would undoubtedly decrease the minima of the proton near PRDa_3, but is not expected to change the relative free energy profiles between the Glu242 and PRDa_3.

It is noteworthy that, as seen in the inserted snapshots in Fig. 4, the conformational isomerization of Glu242 occurs during the proton translocation. In the initial state of proton transfer, the COOH group occupies a conformation with the unpaired oxygen pointing up towards the solvated excess proton. After the proton transfer, Glu242 reverts to its position in the crystal structure, forming a hydrogen bond with the sulfur of Met71 (not shown). The conformational changes of the Glu242 residue may account for the switch and reestablishment of an alternative proton linkage between the D-channel and the active sites. In addition, during the process of proton migration the PRDa_3 side chain swings downwards and establishes a hydrogen-bond connection with the excess proton, and this hydrogen-bond interaction may be a contributing factor to the favorable free energy.

4. Conclusions

One of the key issues to address in CcO's proton pumping mechanism is how PT from Glu242 to the proton-loading site and beyond is coupled to the electron transfer. In this paper, we have examined the dynamics of the protein environment and an explicit excess proton near the putative proton-loading site, the PRDa_3, and also their sensitivity to the different heme and Cu_B oxidation states. The MS-EVB2 simulation results provide clear evidence supporting the view that the reduction of heme *a* induces the conformational reorientation of the PRDa_3 group and that this process subsequently aids in the proton translocation from Glu242 to the PRDa_3. This is potentially the initial step in the proton pumping process that enables, via the increased positive charge of PRDa_3, electron transfer from heme *a* to the binuclear center. Thus, our simulation results favor the mechanism in which transfer of pumped proton precedes the electron transfer to the binuclear center [32,33]. It should be noted that the calculations reported in the present study entirely focus on the initial proton pumping process between Glu242 and the $PRDa_3$ group and do not address the entire enzymatic cycle. In particular, the calculations do not provide information on the chemical pathway between Glu242 and the binuclear center, which demands the characterization of alternative charge/redox states of the binuclear center and many other key groups at various stages of the catalytic cycle.

The key role of the low-spin heme *a* in proton pumping has been proposed previously from experimental investigations of redox-coupled proton movement in the enzyme [34] and careful examination of the high-resolution crystal structures of both the fully oxidized and reduced enzymes [6,35]. Nevertheless, the previous proposal by Tsukihara et al. [6,35,36] suggested the proton pumping event, driven by the oxidation state of heme *a*, occurs through a so-called H-pathway that leads from Arg38 to the mitochondrial intermembrane space via a hydrogen-bond network and ends at the functionally important Asp51. In this paper, under the assumption of the Arg438/PRDa_3 pair being the initial proton-loading site, our simulations focused on the proton pumping pathway between Glu242 and PRDa_3, and have shown no indication of the role of the H- pathway. The data presented in this study also give no indication of the route by which the protons are released from PRDa_3 to the extracellular side. It is conceivable that PRDa_3 may undergo a conformational change and facilitate proton movement to the region above the heme propionates. Results from electrostatic calculations suggest that in the large hydrophilic region at the interface of subunits I and II there is an assembly of interacting acidic groups that could function as proton-shuttling groups [20]. Thus this region has been suggested to provide a proton storage area and part of the exit pathway.

The study of proton pumping in CcO clearly merits further careful examination in the future. To achieve an even greater understanding of the proton pumping mechanism, it is necessary to extend the present MS-EVB simulation model for CcO to include the possible protonation/deprotonation of ionizable residues that play a direct role in proton translocation, such as Glu242 and the D-propionate of heme a_3 group. Future work will be focused on developing accurate parameter for such key protonatable groups and on calculating their pK_a shifts that may arise during the enzymatic cycle.

Acknowledgements

This research was supported by a grant from the National Institutes of Health (R01 GM053148). Helpful discussions with Dr. Jessica M. J. Swanson are gratefully acknowledged. The computations reported in this paper were carried out with allocations of computer time from the National Center for Supercomputing Applications.

References

[1] A. Puustinen, M. Wikström, Proton exit from the heme-copper oxidase of *Escherichia coli*, Proc. Natl. Acad. Sci. U. S. A. 96 (1999) 35–37.
[2] J. Qian, D.A. Mills, L. Geren, K. Wang, C.W. Hoganson, B. Schmidt, C. Hiser, G.T. Babcock, B. Durham, F. Millett, S. Ferguson-Miller, Role of the conserved arginine pair in proton and electron transfer in cytochrome *c* oxidase, Biochemistry 43 (2004) 5748–5756.
[3] D.A. Mills, L. Geren, C. Hiser, B. Schmidt, B. Durham, F. Millett, S. Ferguson-Miller, An arginine to lysine mutation in the vicinity of the heme propionates affects the redox potentials of the hemes and associated electron and proton transfer in cytochrome *c* oxidase, Biochemistry 44 (2005) 10457–10465.
[4] S. Yoshikawa, K. Shinzawa-Itoh, R. Nakashima, R. Yaono, E. Yamashita, N. Inoue, M. Yao, M.J. Fei, C.P. Libeu, T. Mizushima, H. Yamaguchi, T.

Tomizaki, T. Tsukihara, Redox-coupled crystal structural changes in bovine heart cytochrome *c* oxidase, Science 280 (1998) 1723–1729.
[5] S. Iwata, C. Ostermeier, B. Ludwig, H. Michel, Structure at 2.8 Å resolution of cytochrome *c* oxidase from *Paracoccus denitrificans*, Nature 376 (1995) 660–669.
[6] T. Tsukihara, K. Shimokata, Y. Katayama, H. Shimada, K. Muramoto, H. Aoyama, M. Mochizuki, K. Shinzawa-Itoh, E. Yamashita, M. Yao, Y. Ishimura, S. Yoshikawa, The low-spin heme of cytochrome *c* oxidase as the driving element of the proton-pumping process, Proc. Natl. Acad. Sci. U. S. A. 100 (2003) 15304–15309.
[7] L. Qin, C. Hiser, A. Mulichak, R.M. Garavito, S. Ferguson-Miller, Identification of conserved lipid/detergent-binding sites in a high-resolution structure of the membrane protein cytochrome *c* oxidase, Proc. Natl. Acad. Sci. U.S. A. 103 (2006) 16117–16122.
[8] I. Hofacker, K. Schulten, Oxygen and proton pathways in cytochrome *c* oxidase, Proteins 30 (1998) 100–107.
[9] S. Riistama, G. Hummer, A. Puustinen, R.B. Dyer, W.H. Woodruff, M. Wikström, Bound water in the proton translocation mechanism of the haem-copper oxidases, FEBS Lett. 414 (1997) 275–280.
[10] X. Zheng, D.M. Medvedev, J. Swanson, A.A. Stuchebrukhov, Computer simulation of water in cytochrome *c* oxidase, Biochim. Biophys. Acta 1557 (2003) 99–107.
[11] S.A. Seibold, D.A. Mills, S. Ferguson-Miller, R.I. Cukier, Water chain formation and possible proton pumping routes in *Rhodobacter sphaeroides* cytochrome *c* oxidase: a molecular dynamics comparison of the wild type and R481K mutant, Biochemistry 44 (2005) 10475–10485.
[12] M. Wikström, C. Ribacka, M. Molin, L. Laakkonen, M. Verkhovsky, A. Puustinen, Gating of proton and water transfer in the respiratory enzyme cytochrome *c* oxidase, Proc. Natl. Acad. Sci. U. S. A. 102 (2005) 10478–10481.
[13] M. Wikström, M.I. Verkhovsky, G. Hummer, Water-gated mechanism of proton translocation by cytochrome *c* oxidase, Biochim. Biophys. Acta 1604 (2003) 61–65.
[14] G.A. Voth, Computer simulation of proton solvation and transport in aqueous and biomolecular systems, Acc. Chem. Res. 39 (2006) 143–150.
[15] J.M. Swanson, C.M. Maupin, H. Chen, M.K. Petersen, J. Xu, Y. Wu, G.A. Voth, Proton solvation and transport in aqueous and biomolecular systems: insights from computer simulations, J. Phys. Chem., B 111 (2007) 4300–4314.
[16] W.L. Smith, R.T. Forester. 2 ed., Central Laboratory of the Research Councils, Daresbury, Warrington, England, 2002.
[17] W.D. Cornell, P. Cieplak, C.I. Bayly, I.R. Gould, K.M. Merz, D.M. Ferguson, D.C. Spellmeyer, T. Fox, J.W. Caldwell, P.A. Kollman, A second generation force field for the simulation of proteins, nucleic acids, and organic molecules, J. Am. Chem. Soc. 117 (1995) 5179–5197.
[18] J. Xu, G.A. Voth, Computer simulation of explicit proton translocation in cytochrome *c* oxidase: the D-pathway, Proc. Natl. Acad. Sci. U. S. A. 102 (2005) 6795–6800.
[19] J. Xu, G.A. Voth, Free energy profiles for H(+) conduction in the D-pathway of cytochrome *c* oxidase: a study of the wild type and N98D mutant enzymes, Biochim. Biophys. Acta 1757 (2006) 852–859.
[20] A. Kannt, C.R. Lancaster, H. Michel, The coupling of electron transfer and proton translocation: electrostatic calculations on *Paracoccus denitrificans* cytochrome *c* oxidase, Biophys. J. 74 (1998) 708–721.
[21] C.I. Bayly, P. Cieplak, W.D. Cornell, P.A. Kollman, A well-behaved electrostatic potential based method using charge restraints for deriving atomic charges: the RESP model, J. Phys. Chem. 97 (1993) 10269–10280.
[22] T.F.J. Day, A.V. Soudackov, M. Cuma, U.W. Schmitt, G.A. Voth, A second generation multistate empirical valence bond model for proton transport in aqueous systems, J. Chem. Phys. 117 (2002) 5839–5849.
[23] B. Roux, The calculation of the potential of mean force using computer simulations, Comp. Phys. Comm. 91 (1995) 275–282.
[24] M.G. Torrie, P.J. Valleau, Monte Carlo free energy estimates using non-Boltzmann sampling: application to the sub-critical Lennard–Jones fluid, Chem. Phys. Lett. 28 (1974) 578–581.
[25] H.J.C. Berendsen, D. van der Spoel, R. Van Drunen, GROMACS: a message-passing parallel molecular dynamics implementation, Comp. Phys. Comm. 91 (1995) 43–56.
[26] E. Lindahl, B. Hess, D. Van der Spoel, Gromacs 3.0: a package for molecular simulation and trajectory analysis. J. Mol. Model 7 (2001) 306–317.
[27] W. Humphrey, A. Dalke, K. Schulten, VMD—Visual molecular dynamics, J. Mol. Graph. 14 (1996) 33–38.
[28] M. Iwaki, P.R. Rich, An IR study of protonation changes associated with heme–heme electron transfer in bovine cytochrome *c* oxidase, J. Am. Chem. Soc. 129 (2007) 2923–2929.
[29] R.M. Nyquist, D. Heitbrink, C. Bolwien, R.B. Gennis, J. Heberle, Direct observation of protonation reactions during the catalytic cycle of cytochrome *c* oxidase, Proc. Natl. Acad. Sci. U. S. A. 100 (2003) 8715–8720.
[30] B.H. McMahon, M. Fabian, F. Tomson, T.P. Causgrove, J.A. Bailey, F.N. Rein, R.B. Dyer, G. Palmer, R.B. Gennis, W.H. Woodruff, FTIR studies of internal proton transfer reactions linked to inter-heme electron transfer in bovine cytochrome *c* oxidase, Biochim. Biophys. Acta 1655 (2004) 321–331.
[31] J. Xu, M.A. Sharpe, L. Qin, S. Ferguson-Miller, G.A. Voth, Storage of an excess proton in the hydrogen-bonded network of the D-pathway of cytochrome *c* oxidase: identification of a protonated water cluster, J. Am. Chem. Soc. 129 (2007) 2910–2913.
[32] I. Belevich, D.A. Bloch, N. Belevich, M. Wikstrom, M.I. Verkhovsky, Exploring the proton pump mechanism of cytochrome *c* oxidase in real time, Proc. Natl. Acad. Sci. U. S. A. 104 (2007) 2685–2690.
[33] I. Belevich, M.I. Verkhovsky, M. Wikstrom, Proton-coupled electron transfer drives the proton pump of cytochrome *c* oxidase, Nature 440 (2006) 829–832.
[34] N. Capitanio, G. Capitanio, D. Boffoli, S. Papa, The proton/electron coupling ratio at heme a and Cu(A) in bovine heart cytochrome *c* oxidase, Biochemistry 39 (2000) 15454–15461.
[35] S. Yoshikawa, K. Muramoto, K. Shinzawa-Itoh, H. Aoyama, T. Tsukihara, K. Shimokata, Y. Katayama, H. Shimada, Proton pumping mechanism of bovine heart cytochrome *c* oxidase, Biochim. Biophys. Acta 1757 (2006) 1110–1116.
[36] K. Shimokata, Y. Katayama, H. Murayama, M. Suematsu, T. Tsukihara, K. Muramoto, H. Aoyama, S. Yoshikawa, H. Shimada, The proton pumping pathway of bovine heart cytochrome *c* oxidase, Proc. Natl. Acad. Sci. U. S. A. 104 (2007) 4200–4205.